

Thermochemistry of Oxygen Transfer between Rhenium and Phosphine Complexes. A Density Functional Study[†]

Philip Gisdakis, Serge Antonczak, and Notker Rösch*

Institut für Physikalische und Theoretische Chemie, Technische Universität München,
D-85747 Garching, Germany

Received June 24, 1999

The thermochemistry of the oxygen transfer from Cp*ReO₃ to PPh₃, recently studied experimentally, has been investigated by density functional (DF) calculations. Both gradient corrected (BP86) and hybrid (B3LYP) DF methods were employed. The goal of the study was twofold. First, we evaluate the accuracy of the computational methodology for describing a transition metal oxygen multiple bond, and we check some assumptions that were made to establish the experimental thermochemistry of this complex transfer reaction. In this way we validate a computational strategy which we apply in the second part to calculate the Re–O bond dissociation energies in the complexes LReO₃, L = CH₃, C₆H₅, Cl, F, OH, and NH₂. A high level of calculation on appropriate models, including enthalpy corrections and solvent effects, is required to compute enthalpy values of all reaction steps in good agreement with experiment. The B3LYP approach with flexible basis sets leads to Re–O bond energies of analogous complexes LReO₃ (L = Cp, Cp*, and CH₃) of 109, 113, and 153 kcal/mol, respectively; the value calculated for L = Cp* agrees very well with the experimentally derived value of 116 kcal/mol. The structure of the complex with L = Cp is similar to that with L = Cp*, but the Re–O bond is slightly more covalent. Overall, oxygen abstraction by PPh₃ including formation of the dimer (LReO₂)₂ is exothermic for L = Cp* and Cp, but endothermic for L = CH₃. The experimentally not characterized dimer (LReO)₂(μ-O)₂ with L = CH₃ is significantly more stable with respect to its monomers than the analogous dimer with L = Cp. This may be due to a direct Re–Re interaction since the metal–metal distance of (CH₃ReO)₂(μ-O)₂ is calculated to be 2.59 Å, but is 3.14 Å for (CpReO)₂(μ-O)₂. The strength of the P–O bond of OPPh₃ is calculated to be 124 kcal/mol, which is somewhat smaller than the most favorable experimental value of 133 kcal/mol.

1. Introduction

Recently, a number of studies, among them experimental as well as theoretical investigations, have been devoted to rhenium oxo and peroxy complexes.^{1–23} Such compounds play an important role in oxygen transfer reactions¹ in which they may act as oxidizing or reducing agents but also as catalysts for several organic and inorganic processes. Complexes of the type LReO₃ can be considered as prototypes for rhenium oxo compounds and as precursors for rhenium peroxy complexes.¹ Indeed, they are involved in several types of reactions, and they feature changes of reactivity depending on the nature of the ligand L. For example, the complexes CpReO₃ and Cp*ReO₃ are quite stable, but exhibit only medium activity as catalysts (Cp = cyclopentadienyl, Cp* = pentamethylcyclopentadienyl).² Nevertheless, Cp*ReO₃,³ first prepared in 1984,⁴ has become a key compound in the synthesis of rhenium oxoalkyl and

oxoaryl species.⁵ Gable et al. have studied alkene extrusion⁷ with diolates and Cp*ReO₃ as products, extending their investigation of diolate cycloreversion in the system Cp*Re(O)(diolate).⁶

A related compound, CH₃ReO₃ (methyltrioxorhenium, MTO) is a versatile species that is catalytically active in various processes, e.g., in olefin metathesis and epoxidation⁸ as well as in aldehyde olefination,⁹ but it also plays a role in Diels–Alder reactions.¹⁰ Among the transition metal compounds active as catalytic oxygen transfer agents, MTO has been proven to be a highly efficient olefin epoxidation catalyst in the presence of

[†] Dedicated to Professor Reinhart Ahlrichs on the occasion of his 60th birthday.

(1) Herrmann, W. A. *J. Organomet. Chem.* **1995**, *500*, 149. (b) Herrmann, W. A.; Kühn, F. E. *Acc. Chem. Res.* **1997**, *30*, 169. (c) Romão, C. C.; Kühn, F. E.; Herrmann, W. A. *Chem. Rev.* **1997**, *97*, 3197.

(2) Herrmann, W. A.; Ladwig, M.; Kiprof, P.; Riede, J. *J. Organomet. Chem.* **1989**, *371*, C13.

(3) Burrell, A. K.; Cotton, F. A.; Daniels, L. M.; Petricek, V. *Inorg. Chem.* **1995**, *34*, 4253.

(4) Herrmann, W. A.; Serrano, R.; Bock, H. *Angew. Chem.* **1984**, *96*, 364. (b) Klahn-Oliva, A. H.; Sutton, D. *Organometallics* **1984**, *3*, 1313.

(5) Bottomley, F.; Sutin, L. *Adv. Organomet. Chem.* **1988**, *28*, 339. (b) Herrmann, W. A. *J. Organomet. Chem.* **1986**, *300*, 111. (c) Herrmann, W. A.; Floel, M.; Kulpe, J.; Felixberger, J. K.; Herdtweck, E. *J. Organomet. Chem.* **1988**, *355*, 297.

(6) Gable, K. P.; Phan, T. N. *J. Am. Chem. Soc.* **1994**, *116*, 833. (b) Gable, K. P.; Juliette, J. J. *J. Am. Chem. Soc.* **1995**, *117*, 955.

(7) Gable, K. P.; Juliette, J. J. *J. Am. Chem. Soc.* **1996**, *118*, 2625.

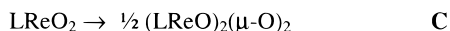
(8) Herrmann, W. A.; Wagner, W.; Flessner, U. N.; Volkhardt, U.; Komber, H. *Angew. Chem., Int. Ed. Engl.* **1991**, *30*, 1636. (b) Herrmann, W. A.; Fischer, R. W.; Marz, D. W. *Angew. Chem., Int. Ed. Engl.* **1991**, *30*, 1638. (c) Herrmann, W. A.; Fischer, R. W.; Scherer, W.; Rauch, M. U. *Angew. Chem., Int. Ed. Engl.* **1993**, *32*, 1157. (d) Al-Ajlouni, A. M.; Espenson, J. H. *J. Am. Chem. Soc.* **1995**, *117*, 9243.

(e) Al-Ajlouni, A. M.; Espenson, J. H. *J. Org. Chem.* **1996**, *61*, 3969.

(9) Herrmann, W. A.; Wang, M. *Angew. Chem.* **1991**, *103*, 1709. (b) Herrmann, W. A.; Wang, M. *Angew. Chem., Int. Ed. Engl.* **1991**, *30*, 1641.

(10) Herrmann, W. A.; Roesky, P. W.; Wang, M.; Scherer, W. *Organometallics* **1994**, *13*, 4531.

Scheme 1



hydrogen peroxide.¹ Apart from these catalysis aspects, it has been shown¹² that CH_3ReO_2 , used as a reducing agent, reacts easily with oxidants such as ClO_4^- to form MTO; in a competing reaction the dinuclear Re(VI) species $\text{CH}_3\text{O}_2\text{Re}-\text{O}-\text{ReO}_2\text{CH}_3$ is formed. MTO, as well as Cp^*ReO_3 , have been structurally characterized by electron diffraction, and they were studied by photoelectron and vibrational spectroscopy.²⁴

Oxorhenium dimers can be obtained by multiple alkylation of simple oxorhenium precursors,¹³ and some of them show activity in olefin epoxidation and olefin metathesis catalysis.¹ The dimer $(\text{Cp}^*\text{ReO})_2(\mu\text{-O})_2$ was studied with particular emphasis. This complex can be obtained through the action of the Lewis base triphenylphosphine on Cp^*ReO_3 . Thereby, an oxo ligand of Cp^*ReO_3 is abstracted in one-to-one fashion; the resulting dioxo moieties dimerize.¹⁴ The reverse reaction, i.e., the fragmentation of such a dimer to form Cp^*ReO_2 or Cp^*ReO_3 ,¹⁵ has recently led to an evaluation of the strength of the rhenium–oxygen double bond, estimated to be 110 kcal/mol.¹⁶ The authors studied the thermodynamics of common reactions between phosphines and rhenium oxo complexes. They evaluated the strength of a Re–O double bond from the reaction energy of the simple reaction $\text{Cp}^*\text{ReO}_3 \rightarrow \text{Cp}^*\text{ReO}_2 + \text{O}$ (see Scheme 1); however, the pertinent thermodynamic cycle involves several steps, e.g., oxidation of phosphine and dimerization of the rhenium complexes. A similar estimate of a Re=O triple bond had previously been proposed¹⁷ on the basis of simple thermodynamic cycles for a rhenium(V) complex. This estimate yields a higher bond strength, by about 25–30 kcal/mol, than that determined recently by Gable and co-workers.¹⁶ A recent computational study demonstrated that Re(I)–O bonds in a rhenium subcarbonyl species bound at a surface defect of magnesium oxide are weaker, but of comparable strength (84 kcal/mol).²⁵ Thus, rhenium, depending on its oxidation state, binds oxygen ligands at different strength.

Application of theoretical methods to rhenium oxo complexes so far focused mainly on structural and spectroscopic properties,^{18,19,24} but was recently extended to the exploration of the mechanisms of peroxi-

dation and oxygen transfer reactions.^{20–23,26} In particular, the mechanism of dihydroxylation by complexes of the type LReO_3 has been studied.^{21,22} The present study also sheds some light on the dihydroxylation of olefins by the MO_3 .²⁶ Experimental data that allow a comparison with calculated results are of great importance for evaluating the predictive power of computational methods. For transition metal compounds there are many structures and some spectroscopic data available for such comparison, but experimental reaction enthalpies are rather scarce.²⁷ Recently, we reviewed how methods based on density functional theory (DFT) can be used to investigate structural and energetic properties of organometallic compounds.²⁸ In the present work we exploit the opportunity that the strength of the rhenium–oxygen double bond in Cp^*ReO_3 has been determined experimentally,¹⁶ and we have calculated the enthalpy changes of all reactions involved in the thermodynamic cycle of Scheme 1.

The goal of the present work is to establish a computational strategy for oxygen transfer and other reactions involving rhenium and related oxo complexes^{20,23} and to assess the effort necessary for achieving satisfactory accuracy. However, a successful comparison of experimental and computational results also lends confidence to estimates or choices among alternative experimental data that sometimes are unavoidable when selecting the experimental database for a complete reaction cycle.¹⁶

We will discuss details of the theoretical strategy and elaborate how the calculated results can be improved in a step-by-step fashion by modifying the “parameters” of the calculations. Computational work begins by choosing models and methods. An appropriate model features all pertinent structural and electronic properties of the target system, yet is of moderate size and thus leads to an acceptable computational effort. Furthermore, a quantum chemical method has to be chosen in combination with an appropriate basis set, and the accuracy of the method has to be evaluated. Calculated reaction energies need to be corrected to yield enthalpy values that allow direct comparison with experiment; also, depending on the system, solvent effects have to be taken into account.

The present work is divided into two parts. First, the reaction system under study (see Scheme 1) is investi-

(11) Zhu, Z.; Espenson, J. H. *J. Am. Chem. Soc.* **1997**, *119*, 3507.

(12) Abu-Omar, M. M.; Espenson, J. H. *Inorg. Chem.* **1995**, *34*, 6239.

(13) Herrmann, W. A.; Watslowik, P.; Kiprof, P. *Chem. Ber.* **1991**, *124*, 1101. (b) Haaland, A.; Verne, H. P.; Volden, H. V.; Herrmann, W. A.; Kiprof, P. *J. Mol. Struct.* **1995**, *352*, 153.

(14) Herrmann, W. A.; Flöel, M.; Kulpe, J.; Felixberger, J. K.; Herdtweck, E. *J. Organomet. Chem.* **1988**, *355*, 297. (b) Herrmann, W. A.; Serrano, R.; Küsthardt, U.; Ziegler, M. L.; Guggolz, E.; Zahn, T. *Angew. Chem., Int. Ed. Engl.* **1984**, *7*, 515. (c) Herrmann, W. A.; Serrano, R.; Küsthardt, Guggolz, E.; Nuber, B.; Ziegler, M. L. *J. Organomet. Chem.* **1985**, *287*, 329.

(15) Gable, K. P.; Juliette, J. J. J.; Gartman, M. A. *Organometallics* **1995**, *14*, 3138.

(16) Gable, K. P.; Juliette, J. J. J.; Li, C.; Nolan, S. P. *Organometallics* **1996**, *15*, 5250.

(17) Conry, R. R.; Mayer, J. M. *Inorg. Chem.* **1990**, *29*, 4862.

(18) Köstlmeier, S.; Häberlen, O. D.; Rösch, N.; Herrmann, W. A.; Solouki, B.; Bock, H. *Organometallics* **1996**, *15*, 1872. (b) Köstlmeier, S.; Pacchioni, G.; Rösch, N. *J. Organomet. Chem.* **1996**, *514*, 111. (c) Köstlmeier, S.; Nasluzov, V. A.; Herrmann, W. A.; Rösch, N. *Organometallics* **1997**, *16*, 1786.

(19) Szyperski, T.; Schwerdtfeger, P. *Angew. Chem., Int. Ed. Engl.* **1989**, *28*, 1228. (b) Wiest, R.; Leininger, T.; Jeung, G.-H.; Bénard, M. *J. Phys. Chem.* **1992**, *96*, 10800.

(20) Gisdakis, P.; Antonczak, S.; Köstlmeier, S.; Herrmann, W. A.; Rösch, N. *Angew. Chem., Int. Ed. Engl.* **1998**, *37*, 2211; *Angew. Chem.* **1998**, *110*, 2333. (b) Gisdakis, P.; Antonczak, S.; Rösch, N. To be published.

(21) Pietsch, M. A.; Russo, T. V.; Murphy, R. B.; Martin, R. L.; Rappe, A. K. *Organometallics* **1998**, *17*, 2716.

(22) Deubel, D. V.; Frenking, G. *J. Am. Chem. Soc.* **1999**, *121*, 2021.

(23) Kühn, F. E.; Santos, A. M.; Roesky, P. W.; Herdtweck, E.; Scherer, W.; Gisdakis, P.; Yudanov, I. V.; Di Valentin, C.; Rösch, N. *Chem. Eur. J.* **1999**, *5*, 3603.

(24) Herrmann, W. A.; Kiprof, P.; Rypdal, K.; Tremmel, J.; Blom, R.; Alberto, R.; Behm, J.; Albach, R. W.; Bock, H.; Solouki, B.; Mink, J.; Lichtenberger, D.; Gruhn, N. E. *J. Am. Chem. Soc.* **1991**, *113*, 65.

(25) Hu, A.; Neyman, K. M.; Staufer, M.; Belling, T.; Gates, B. C.; Rösch, N. *J. Am. Chem. Soc.* **1999**, *121*, 4522.

(26) Gisdakis, P.; Rösch, N. To be published.

gated computationally using various DF methods. A variety of computational “parameters” have been tested, e.g., basis sets without and with polarization functions, various contraction schemes on the metal center, different exchange–correlation functionals (B3LYP, BP86, and RPBE), and different levels of computation for describing the transition metal center (effective core potentials as well as a scalar-relativistic all-electron description). The corresponding computational results are compared to experimental energy data, taking enthalpy corrections (including zero-point energies) and solvent effects into account. In this way an accurate strategy for calculating bond energies of reactions of transition metal oxo and peroxy complexes is established. In a second step, we apply this strategy to explore and compare Re–O bond energies in compounds of the type LReO_3 with $\text{L} = \text{CH}_3, \text{C}_6\text{H}_5, \text{Cl}, \text{F}, \text{OH}, \text{NH}_2, \text{Cp},$ and Cp^* . Furthermore, we will evaluate the energies of dimerization for the reduced molecules LReO_2 for $\text{L} = \text{CH}_3, \text{Cp},$ and Cp^* .

2. Computational Details, Models

Methods. Chemical properties of transition metal complexes can be calculated with appropriate accuracy and in a very efficient fashion by employing DF methods in combination with an effective core potential (ECP) approach.^{28,28} Although commonly available ECP parameters and basis sets are generated using Hartree–Fock methodology, they have been shown to be also applicable to DF methods.³⁰ Basis sets have to be chosen carefully. The standard basis set LANL2DZ³¹ available in the Gaussian94 program³² is a combination of a double- ζ basis set without polarization functions for first-row elements and Los Alamos ECPs with a double- ζ basis set on heavy atoms, including phosphorus. Lack of polarization functions on elements such as H, C, O, and P leads to inappropriate structural and energy results, as will be shown below. A detailed analysis of such properties should be based on an improved description where polarization functions are included at least for the main group elements.²⁹ The present work will show how calculated structures and reaction energies of oxygen transfer from Cp^*ReO_3 to triphenylphosphine PPh_3 converge to experimental values when the basis set is systematically improved. Table 1 provides an overview of the various basis sets employed in this comparative study. A Roman numeral shall indicate the overall quality of the basis set: I, “minimal” double- ζ description without polarization functions; II, intermediate quality with polarization functions for main group elements only (6-311G(d,p)³³); III, basis set with polarization functions for all elements. Note that basis sets II and III are identical as far as the main group elements are concerned. Variations in transition metal basis sets II and III are denoted by a suffix: a, standard LANL2DZ basis set; b, modified LANL2DZ basis, “de-contracted” as described by Frenking et al.²⁹ We will show that there are geometrical changes when the basis set is improved from I to IIa, while the further decontraction of the metal basis set leading to IIb does not alter the geometries much, but changes the energetics to some extent.

(27) Irikura, K. K.; Frurip, D. J., Eds. *Computational Thermochemistry: Prediction and Estimation of Molecular Thermodynamics*; ACS Symposium Series No. 677; American Chemical Society: Washington, DC, 1998.

(28) Görling, A.; Trickey, S. B.; Gisdakis, P.; Rösch, N. In *Organometallic Bonding and Reactivity*; Brown, J. M., Hofmann, P., Eds.; Topics in Organometallic Chemistry, Vol. 4; Springer: Heidelberg, 1999; p 109.

(29) Frenking, G.; Antes, I.; Böhme, M.; Dapprich, S.; Ehlers, A. W.; Jonas, V.; Neuhaus, A.; Otto, M.; Stegmann, R.; Veldkamp, A.; Vyboshchikov, S. F. In *Reviews in Computational Chemistry*; Lipkowitz, K. B., Boyd, D. B., Eds.; VCH: New York, 1996; Vol. 8, p 63.

Table 1. Basis Sets Used in the Present Study (in combination with LANL2^a effective core potential, ECP, for Re)^b

	transition metal	main group elements
I	(341/321/21) ^a	D95V ^a
IIa	(341/321/21)	6-311G(d,p) ^c
IIb	(441/2111/21) ^d	6-311G(d,p)
IIIa	(341/321/21/11) ^e	6-311G(d,p)
IIIb	(441/2111/21/11) ^{d,e}	6-311G(d,p)

^a Ref 31. Phosphorus described by ECP of LANL1DZ. ^b Addition of three d-type polarization exponents on P (1.0722, 0.4226, and 0.1666)³⁵ is indicated by a prime, e.g. IIIb'. ^c Ref 33. ^d Contraction modified according to ref 29. ^e Re f-type polarization exponents 0.5895 and 0.2683 (see text).

The two exponents of the Re f-type polarization functions (basis sets III), 0.5895 and 0.2683, were determined in two steps. First, radial expectation values of the three most diffuse Re d basis functions were matched by f basis functions, then the resulting three exponents were reduced to two by taking the geometric means between two successive pairs. The effect of these two f polarization exponents was compared with the one f exponent proposed previously (0.869).³⁴ The total energy values of CpReO_3 and CpReO_2 are lowered by 12.8 and 7.4 kcal/mol, respectively, when two instead of one exponent are used; the resulting energy difference will turn out to be of importance in a comparison with the experimental energy of oxygen abstraction.

A prime (e.g., II') shall be used to denote a more flexible set of d polarization functions for phosphorus. The three d polarization exponents of phosphorus (1.0722, 0.4226, and 0.1666), which replace the original exponent (0.55) of the 6-311G(d,p) basis set, were taken from Widmark et al.³⁵

We shall employ the common notation B2/B1 to denote the result of a single-point energy calculation with basis set B2 using a geometry optimized with basis set B1. To check whether the rather small LANL2DZ basis set for Re (Table 1, basis set I) is suitable for geometry optimization, we carefully compared pertinent structural parameters and energies at the levels I and IIIb'/I with results obtained from calculations at levels IIb and IIIb'/IIb (e.g., Table 2). We will discuss basis sets below in more detail. Here, we note that overall the combination strategy IIIb'/IIb was found to be very satisfactory, although level IIIb'/I provides useful results for rhenium oxo complexes at a reasonable cost. However, this level is not recommended in general since the applicability of basis set I is too limited; for example, it is not adequate for describing peroxy complexes and their reactivity.^{20,36}

The B3LYP³⁹ hybrid density functional method was used for all geometry optimizations and in most of the single-point energy calculations. It mixes the gradient-corrected exchange energy functional of Becke^{40a} with exactly evaluated single-determinant exchange and combines it with the gradient-corrected correlation energy functional as suggested by Lee, Yang, and Parr.^{39b} To explore the effect of a different exchange–correlation functional, we also used the popular⁴¹ gradient-

(30) Russo, T. V.; Martin, R. L.; Hay, P. J. *J. Phys. Chem.* **1995**, *99*, 17085.

(31) Dunning, T. H.; Hay, P. J. In *Modern Theoretical Chemistry*; Schaefer H. F., III, Ed.; Plenum Press: New York, 1976; Vol. 3, p 1. (b) Hay, P. J.; Wadt, W. R. *J. Chem. Phys.* **1985**, *82*, 299.

(32) Frisch, M. J.; Trucks, G. W.; Schlegel, H. B.; Gill, P. M. W.; Johnson, B. G.; Robb, M. A.; Cheeseman, J. R.; Keith, T.; Petersson, G. A.; Montgomery, J. A.; Raghavachari, K.; Al-Laham, M. A.; Zakrzewski, V. G.; Ortiz, J. V.; Foresman, J. B.; Cioslowski, J.; Stefanov, B. B.; Nanayakkara, A.; Challacombe, M.; Peng, C. Y.; Ayala, P. Y.; Chen, W.; Wong, M. W.; Andres, J. L.; Replogle, E. S.; Gomperts, R.; Martin, R. L.; Fox, D. J.; Binkley, J. S.; Defrees, D. J.; Baker, J.; Stewart, J. P.; Head-Gordon, M.; Gonzalez, C.; Pople, J. A. *Gaussian 94*, Revision D.4; Gaussian, Inc.: Pittsburgh, PA, 1995.

(33) Krishnan, R.; Binkley, J.; Seeger, R. Pople, J. *J. Chem. Phys.* **1980**, *72*, 650. (b) McLean, A.; Chandler, G. *J. Chem. Phys.* **1980**, *72*, 5639.

Table 2. Comparison of Experimental Energies (in kcal/mol) of the Reaction Steps of Scheme 1 with Computational Results Obtained with Various Basis Sets^a and Exchange–Correlation Functionals

	L = Cp						L = Cp*					
	B3LYP				BP86		RPBE	B3LYP		BP86	Exp.1 ^b	Exp.2 ^c
	I	IIb	IIIb/I	IIIb/IIb	IIIb/IIb	AE/IIb	AE/IIb	IIIb/IIb	IIIb/IIb			
A	89.2	97.3	108.6	109.2	129.4	124.5	119.2	113.4	133.1	114.1	117.5	
B	-76.3	-117.9	-116.1	-123.8	-131.5	-127.1	-123.5	-123.8	-131.5	-132.0	-135.4	
C	-11.8	-10.4	-9.4	-9.4	-11.3	-10.9	-7.9	-9.5	-11.3 ^d	-11.0	-11.0	
D	1.1	-31.0	-16.9	-24.0	-13.4	-13.5	-12.2	-19.9	-9.7	-28.9	-28.9	

^a See Table 1. AE: all-electron calculation (see text). ^b Reaction energies based on data set Exp.1 (see Table 8) including the P–O bond energy (**B**) of ref 50. ^c Reaction energies based on data set Exp.2 (see Table 8) including the P–O bond energy (**B**) of ref 16. ^d Estimated by the value for L = Cp.

corrected BP86 functional⁴⁰ at the level IIIb/IIb. Finally, we estimated effects of the ECP approach by comparison with results of a scalar-relativistic all-electron description afforded by the LCGTO-DF method,^{42,43} where the BP86 functional and a recently proposed modification⁴⁴ of the gradient-corrected functional of Perdew, Burke, and Ernzerhof⁴⁵ (RPBE) were used in combination with flexible basis sets.⁴⁶

To achieve a better comparison with experimental values of reaction enthalpies, harmonic vibrational frequencies⁴⁷ of model compounds were calculated (at levels I and IIb) in order to apply enthalpy corrections to computed calculated reaction energy values. For convenience, we also apply enthalpy corrections (including zero-point energies) to experimental reaction enthalpy values ΔH so that the discussion of various methodological aspects can be based on reaction energies throughout.

Furthermore, solvent effects were estimated in single-point calculations where an averaged effect of the solvent was taken into account using a “polarizable continuum” model in a self-consistent reaction field approach.⁴⁸ Thereby, the solute is assumed to be located in an ellipsoidal cavity created in a dielectric continuum; here, the dielectric constant of toluene was chosen ($\epsilon = 2.38$ for $T = 298$ K). In this model approach to solvent effects, the charge distribution of the solute is allowed to polarize the dielectric continuum environment, which, in turn, creates an electric field inside the cavity. This electric field is determined via a multipole expansion of the solute charge distribution.

All calculations (except where noted) were carried out with the program Gaussian94/DFT³² in combination with the SCR-FPAC package⁴⁹ for the studies of solvent effects.

Models. To check the DF methods applied in a benchmark fashion, we calculated the reactions presented Scheme 1 for the experimentally used ligand L = Cp*. Then we studied whether the ligand Cp* can be modeled by the computationally less demanding ligand Cp. To keep the computational effort manageable, we performed the analysis of the effects of different computational strategies for complexes with a Cp model ligand. The influence of different ligands L on the Re–O bond was also investigated for model systems with L = CH₃, C₆H₅, Cl, Fl, OH, and NH₂. Since stabilization of the LReO₂ fragment plays an important role in the oxygen abstraction

Table 3. Calculated^a Bond Distances (in Å), NBO Charges q (in e), and Dipole Moments μ (in D) of the Rhenium Complexes Involved in Reactions A, C, and D

	(Cp*ReO) ₂ (μ -O) ₂		Cp*ReO ₃		Cp*ReO ₂
	calc	expt ^b	calc	expt ^c	calc
Re1–C1	2.18	2.19	2.48	2.32	2.32
Re1–C2	2.26	2.24	2.43	2.37	2.30
Re1–C3	2.55	2.44	2.44	2.36	2.45
Re1–O1	1.71	1.69	1.74	1.73	1.72
Re1–O2	1.98	1.96	1.74	1.74	1.73
Re1–Re2	3.16	3.14			
C1–C2	1.45	1.44	1.43	1.43	1.43
C2–C3	1.46	1.44	1.44	1.42	1.46
C3–C3'	1.39	1.40	1.43	1.44	1.40
$q(\text{Cp}^*)^d$	0.09 (0.25)		0.0 (–0.03)		–0.07 (–0.08)
$q(\text{Re})^d$	1.21 (0.85)		1.83 (1.91)		1.25 (1.29)
$q(\text{O1})^{d,e}$	–0.58 (–0.47)		–0.61 (–0.62)		–0.58 (–0.59)
$q(\text{O2})^{d,e}$	–0.72 (–0.63)		–0.61 (–0.63)		–0.60 (–0.62)
μ^d	0.0 (0.0)		6.70 (6.49)		6.25 (6.11)

^a B3LYP method with basis set IIb. ^b Ref 14a. ^c Ref 3. ^d Values calculated at level IIIb/IIb in parentheses. ^e See Figure 1 for atom labels.

reaction, we studied two possible mechanisms for systems with L = CH₃ and Cp, dimerization.

Experimental oxygen transfer reactions involving various phosphine and phosphine oxide compounds^{16,50} show a notable dependence of the reaction energies on the nature of the phosphine substituents. Therefore, we decided to employ triphenylphosphine, PPh₃, and triphenylphosphine oxide, OPPh₃, rather than model phosphines. The structures of these phosphine compounds were fully optimized in C₃ symmetry and were used in the energy analysis of the reactions studied. However, model phosphines such as PH₃ and PMe₃ and the corresponding oxides were also calculated, in particular to estimate solvent effects and enthalpy correction terms on the formation energy of the P–O bond. Not unexpectedly, these optimized model structures exhibit noticeable differences compared to triphenylphosphine and triphenylphosphine oxide.

Finally, we emphasize that we evaluated the thermochemistry of the reactions presented in Scheme 1 on fully optimized structures, namely, those of the rhenium complexes LReO₃, LReO₂, and (LReO)₂(μ -O)₂ as well as those of the compounds PPh₃ and OPPh₃.

3. Results and Discussion

3.1. Structures. Rhenium Complexes. A direct comparison between experimental structures of (Cp*ReO)₂(μ -O)₂ and Cp*ReO₃ and geometries optimized at level B3LYP-IIb (see Table 3) shows that this level of calculation adequately reproduces the experimental structures. Nevertheless, some differences are worth discussing. Before analyzing them, we would like to point out that the experimental structure of the dimer

(34) Ehlers, A. W.; Böhme, M.; Dapprich, S.; Gobbi, A.; Höllwarth, A.; Jonas, V.; Köhler, K. F.; Stegmann, R.; Veldkamp, A.; Frenking, G. *Chem. Phys. Lett.* **1993**, *208*, 111.

(35) Widmark P.-O.; Persson B. J.; Roos B. O. *Theor. Chim. Acta* **1991**, *79*, 419.

(36) Cf. the C–O bond lengths in transition states of the [2+3] cycloaddition of ethylene to OsO₄: 2.37 Å for LANL2DZ on all elements³⁷ vs 2.08 Å for LANL2DZ on Os and 6-31G(d) on C, H, O.³⁸

(37) Dapprich, S.; Ujaque, G.; Maseras, F.; Lledos, A.; Musaeu, D. G.; Morokuma, K. *J. Am. Chem. Soc.* **1996**, *118*, 11660.

(38) Pidun, U.; Boehme, C.; Frenking, G. *Angew. Chem., Int. Ed. Engl.* **1996**, *35*, 2817.

(39) Becke, A. D. *J. Chem. Phys.* **1993**, *98*, 5648. (b) Lee, C.; Yang, W.; Parr, R. G. *Phys. Rev. B* **1988**, *37*, 785.

(40) Becke, A. D. *Phys. Rev. A* **1988**, *38*, 3098. (b) Perdew, J. P. *Phys. Rev. B* **1986**, *33*, 8822.

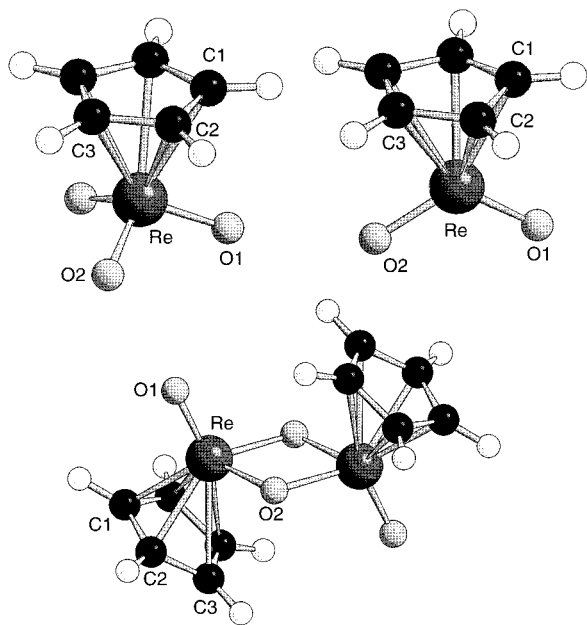


Figure 1. Calculated structures of Cp^*ReO_3 , Cp^*ReO_2 (both in C_s symmetry) and $(\text{Cp}^*\text{ReO})_2(\mu\text{-O})_2$ (C_{2h} symmetry). Labels with primes discriminate symmetry equivalent atoms.

presented in Table 3 is extracted from an X-ray analysis^{14b} with two nonequivalent $(\text{Cp}^*\text{ReO})_2(\mu\text{-O})_2$ moieties per unit cell and that the two structure determinations^{3,24} performed on the complex Cp^*ReO_3 disagree in some aspects.

Small distortions of the experimental structure of the dimer $(\text{Cp}^*\text{ReO})_2(\mu\text{-O})_2$ may be due to two crystal water molecules which interact with the bridging oxygen of the dimer through hydrogen bonds. Although they do not coordinate to the metal centers, these water molecules are expected to affect the Re–O bonds. In the calculations, we optimized the structure of $(\text{Cp}^*\text{ReO})_2(\mu\text{-O})_2$ for the gas phase, applying C_{2h} symmetry constraints (Figure 1); crystal packing effects are likely responsible for the lower experimental symmetry.^{14b} The most important bond length differences between the crystallographic and the calculated structures are found for the coordination of the Cp^* ring to the metal center. In particular, the bond Re1–C3 (see Figure 1) is calculated to be 2.55 Å, 0.12 Å longer than the corresponding experimental distance. All other differences between experimental and calculated structures of the dimer are rather small, and general trends are well represented. Both experimental and calculated structures exhibit a rhenium oxygen double bond (calc 1.71 Å) and two rhenium oxygen single bonds (calc 1.98 Å), the latter being involved in the bridges between the rhenium atoms. The distance between the two metal centers is relatively long, 3.16 Å calculated and 3.14 Å experimental.

In the complex Cp^*ReO_3 , the calculated Re–C bond lengths are noticeably longer, by 0.06–0.16 Å, than those obtained in an apparently complicated X-ray analysis.³ The calculations agree somewhat better with the results of an electron diffraction analysis with deviations of 0.03–0.08 Å.²⁴ Comparison of the calculated structures of Cp^*ReO_3 and Cp^*ReO_2 , both of C_s symmetry, leads to two noteworthy findings. First, both oxygen atoms of Cp^*ReO_2 lie in the mirror plane of the

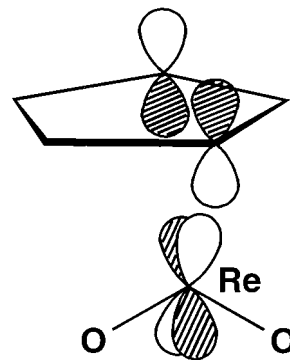


Figure 2. Simplified representation of the metal–Cp interaction in Cp^*ReO_2 : LUMO of ReO_2^+ and one of the filled π orbitals of the distorted Cp ring.

molecule (see Figure 1), while Cp^*ReO_3 has a “piano stool” shape with three Re–O bonds of equal length. The Re–O bond lengths of both molecules are about 1.72 Å, a typical value.^{1,3,14a} Furthermore, in the complex Cp^*ReO_2 , two quite distinct Re–C bond distances are found, differing by 0.15 Å, compared to Cp^*ReO_3 , where the Re–C distances differ among each other by at most 0.05 Å; the experimental variation is also 0.05 Å.³ These changes in the Re–C bonds are accompanied by a shift of the rhenium atom from a position approximately under the center of the Cp^* ring in Cp^*ReO_3 toward the side of an allylic moiety formed by the carbon atoms C1, C2, and C2' in Cp^*ReO_2 . In fact, when going from Cp^*ReO_3 to Cp^*ReO_2 , one notes two types of C–C bond distance alterations: the distance C3–C3' decreases slightly, while the other C–C bonds increase or remain unchanged. These C–C distance changes are rather small, but can also be observed by comparing the experimental structures of Cp^*ReO_3 and the dimer. The shortened C3=C3' bond acquires double-bond character and can thus act as an electron donor to the metal, whereas the remaining part of the cyclopentadienyl ring may be viewed as an allylic moiety.

The structure of the molecule Cp^*ReO_2 and the relative orientation of the moiety ReO_2^+ in particular can be rationalized by the Cp–metal orbital interaction. The formal oxidation state of the metal center changes from Re(VII) in Cp^*ReO_3 to Re(V) in Cp^*ReO_2 . Thus, whereas the ReO_3^+ fragment (C_{3v} symmetry) is a d^0 complex, an Re sd hybrid orbital (of a_1 symmetry) is occupied in the moiety ReO_2^+ (C_{2v} symmetry), which, however, is not significantly involved in the bonding of the Cp ring. Rather, the LUMO of ReO_2^+ , a d orbital antisymmetric with respect to the reflection plane O–Re–O, interacts with the corresponding (filled) symmetry partner of the $e(\pi)$ set of the Cp ring (see Figure 2). This π MO of Cp has larger coefficients on C2 and C2' (cf. Figure 1 for the atom labeling), inducing a shift of the Re atom away from a central position underneath the Cp ring. Accordingly, the LUMO of ReO_2^+ interacts with the nonbonding π orbital of the allylic moiety of the Cp ring (Figure 2).

The substitution of permethylated cyclopentadienyl Cp^* by a simple Cp ligand has only small effects on the structures of the various complexes; bond distances change by less than 0.02 Å. The largest modification is found in the structure of Cp^*ReO_3 optimized at level IIIb, where the bonds Re–C2 and Re–C3 of Cp^*ReO_3 are about 0.04 Å shorter than in Cp^*ReO_3 ; the distance Re–

Table 4. Calculated^a Structural Parameters (in Å, deg) and Dipole Moments μ (in D) of the Phosphorus Compounds of the Reactions B and D

	PPh ₃		OPPh ₃	
	calc	expt ^b	calc	expt ^c
P–C	1.85	1.83	1.82	1.80
P–O			1.50	1.49
C–P–C	102.4		106.2	
C–P–Z ^d	115.9		112.6	
ΔE	1.46 (1.47)		4.23 (4.12)	

^a B3LYP method and basis set II. ^b Ref 52. ^c Ref 53. ^d Z refers to the symmetry axis of the molecule, along the P–O bond in the case of OPPh₃.

C1 expands slightly, by 0.01 Å, when Cp* is replaced by Cp. These changes reflect the increased electron donor capability of the ligand Cp*.⁵¹

The differences between experimental and calculated Re–C bond lengths discussed above may in part be caused by packing effects in the crystal structure since the ring–metal bonds are rather weak in general. As an estimate, we mention the fairly small energy difference of about 4 kcal/mol that is calculated at level IIb between the fully optimized structure of CpReO₂ and an idealized structure optimized by constraining all Re–C distances to be equal to each other. CpReO₂ was chosen for this comparison since the Re center is in the same formal oxidation state V as in the dimer (CpReO)₂(μ -O)₂. Similarly, when all Re–C bonds of CpReO₃ are fixed to the average value of the experimental structure, 2.36 Å, the calculated energy increases by only 3 kcal/mol.

The f polarization functions in the Re basis set do not significantly affect the NBO atomic charges, but they change the values of the dipole moment of Cp*ReO₃ and Cp*ReO₂ when going from level IIb to IIIb/IIb. At level IIIb/IIb, the dipole moments of Cp*ReO₃ and Cp*ReO₂ are quite comparable, 6.49 and 6.11 D, respectively, with the charge separation in Cp*ReO₂ being somewhat smaller. (The corresponding values for CpReO₃ and CpReO₂ are 5.50 and 5.18 D, respectively.) The dipole moment of the dimer (CpReO)₂(μ -O)₂ vanishes since its structure exhibits an inversion center.

A comparison of the three rhenium oxo complexes reveals that a partial “decontraction” of the metal basis set with the basis sets IIa and IIb or even a totally decontracted metal basis set yields essentially the same optimized geometries; bond distances change at most by 0.01 Å.

As indicated above, geometries of the Re complexes calculated at level I (LANL2DZ) also fit experimental values rather well, although bond lengths are consistently longer than those of level IIb, by about 0.02–0.05 Å. Apparently, these oxo complexes do not contain bonds that are difficult to describe, such as hypervalent bonds in the phosphine oxides, to be discussed below, or bonds in peroxo complexes.²⁰

Phosphine Complexes. The structures of the molecules triphenylphosphine, PPh₃, and triphenylphosphine oxide, OPPh₃, were optimized with basis sets I and II, applying C₃ symmetry constraints. Pertinent geometry parameters are compiled in Table 4. One notes small changes in bond lengths when going from PPh₃ to OPPh₃; for example, the P–C bond shortens by 0.03 Å. This change fits experimental data where the P–C

Table 5. Calculated^a Dipole Moment μ (in D) and P–O Bond Length (in Å) of Model Phosphine Compounds for Various Basis Sets^b

	PH ₃	OPH ₃		PMe ₃	OPMe ₃	
	μ	μ	d(O–P)	μ	μ	d(O–P)
I	1.30	4.82	1.62	1.41	5.34	1.62
II	0.77	3.80	1.49	1.40	4.48	1.50
II'/II	0.52	3.55	1.49 ^c	1.35	4.30	1.50 ^c
expt	0.58 ^d			1.19 ^e		

^a B3LYP method. ^b See Table 1. ^c Not optimized. ^d Ref 57. ^e Ref 59.

bond length exhibits a corresponding decrease of 0.025–0.036 Å.^{52,53} This oxidation of the phosphorus center leads to a decrease of the angle C_XPZ between the P–C bonds and the symmetry axis Z of the molecule (in the case of OPPh₃ the phosphorus and oxygen centers define this axis). In OPPh₃ the calculated values of the P–C and the P–O bond lengths agree quite well with experimental data (Table 4).⁵³ P–O bond lengths of hypervalent compounds⁵⁴ fall in the range 1.47–1.49 Å, while typical P–O single bonds, such as a bridging bond in P₄O₁₀, are about 1.60 Å.⁵⁵ Optimization of OPPh₃ with basis set I yields an inadequate P–O distance of 1.62 Å (see also the corresponding results for model phosphines; Table 5).

Clearly, care is required when a hypervalent P–O bond is to be described as shown by the present results for several model phosphine compounds as well as by several other studies.^{35,54,56–58} In Table 5, we compare the P–O bond length and the dipole moment calculated for PH₃, OPH₃, PMe₃, and OPMe₃ using various basis sets. These results demonstrate the necessity of including d polarization functions in the basis set of phosphorus. Basis set I, without polarization functions, does not yield an adequate description of the electronic structure of such a hypervalent compound. Optimized geometries at level II exhibit acceptable P–O bond lengths as obtained previously for OPPh₃; d polarization functions on the phosphorus atom (level II') cause only small changes of the P–O bond length, by 0.01 Å. Previous

(41) Ziegler, T. *Chem. Rev.* **1991**, *91*, 651.

(42) Häberlen, O. D.; Rösch, N. *Chem. Phys. Lett.* **1992**, *199*, 491. (b) Dunlap, B. I.; Rösch, N. *Adv. Quantum Chem.* **1990**, *21*, 317. (c) Rösch, N.; Krüger, S.; Mayer, M.; Nasluzov, V. A. In *Recent Developments and Applications of Modern Density Functional Theory*; Seminario, J. M., Ed.; Elsevier: Amsterdam, 1996; p 497.

(43) Matveev, A.; Stauffer, M.; Mayer, M.; Rösch, N. *Int. J. Quantum Chem.*, in press.

(44) Hammer, B.; Hansen, L. B.; Norksov, J. K. *Phys. Rev. B* **1999**, *59*, 7413.

(45) Perdew, J. P.; Burke, K.; Ernzerhof, M. *Phys. Rev. Lett.* **1996**, *77*, 3865.

(46) Basis sets for the all-electron calculations. Re (21s17p12d7f) → [9s8p5d2f]: Gropen, O. *J. Comput. Chem.* **1987**, *8*, 982. P (12s9p3d) → [6s5p3d]: Veillard, A. *Theor. Chim. Acta* **1968**, *12*, 405. Reference 35. C, O (9s5p1d) → [5s4p1d], H (6s1p) → [4s1p]: van Duijneveldt, F. B. IBM Research Report Nr. RJ 945, 1971. Huzinaga, S. *Gaussian Basis Sets for Molecular Calculations*; Elsevier: New York, 1984.

(47) Hehre, W. J.; Radom, L.; Schleyer, P. v. R.; Pople, J. A. *Ab Initio Molecular Orbital Theory*; Wiley: New York, 1986.

(48) Rinaldi, D.; Ruiz-López, M. F.; Rivail, J.-L. *J. Chem. Phys.* **1983**, *78*, 834. (b) Rinaldi, D.; Rivail, J.-L.; Rguini, N. *J. Comput. Chem.* **1992**, *13*, 675.

(49) Rinaldi, D.; Pappalardo, R. R. *SCRFPAC*; Quantum Chemistry Program Exchange: Indiana University, Bloomington, 1992; no. 622.

(50) Holm, R. H.; Donahue, J. P. *Polyhedron* **1993**, *12*, 571.

(51) Elschenbroich, C.; Salzer, A. *Organometallics*; Teubner: Stuttgart, 1990; p 62.

(52) Daly, J. J. *J. Chem. Soc.* **1964**, 3799.

(53) Spek, A. L. *Acta Crystallogr., Sect. C* **1987**, *43*, 1233. (b) Ruban, G.; Zabel, V. *Cryst. Struct. Commun.* **1976**, *5*, 671 (c) Brock, C. P.; Scheizer, W. B.; Dunitz, J. D. *J. Am. Chem. Soc.* **1985**, *107*, 6964.

Table 6. Energies ΔE of the P–O Bond in Model Phosphine Oxides and Temperature and Zero-Point Energy Corrections $\Delta^2 H$ and Solvent Effects $\Delta^2 E$ (in kcal/mol) Calculated with the B3LYP Method and Basis Sets II and II'/II

	PH ₃ + O → OPH ₃		PMe ₃ + O → OPMe ₃		PPh ₃ + O → OPPh ₃	
	II	II'/II	II	II'/II	II	II'/II
ΔE	-97.3	-105.2	-121.4	-127.6	-117.9	-123.8
$\Delta^2 H$	+3.0	+2.9	+1.9	+1.5	+2.1	
$\Delta^2 E(\text{Solv})$	-3.7	-2.6	-3.3	-3.5		

studies⁵⁶ have shown that extravalence d basis functions on phosphorus are required for obtaining correct bond lengths and bond energies of hypervalent phosphine complexes. It is now well accepted⁵⁶ that in hypervalent molecules d-type basis functions are to be considered as polarization functions that are essential to enable an efficient description of the rapidly varying internuclear molecular potential, rather than to make a covalent contribution.^{57,58}

Inspection of Table 5 demonstrates that d polarization functions on phosphorus have a noticeable influence on the calculated dipole moments of model phosphine compounds. Comparing with experimental values^{59,60} for both PH₃ and PMe₃, one notes that introduction of additional d polarization functions on the phosphorus center (level II') leads to improved agreement of calculated and experimental values of the dipole moment (Table 5). Single-point calculations at level II'/II yield dipole moments very close to those obtained at level II'; deviations are at most 0.04 D (for OPMe₃).

Taking into consideration all experimental and calculated data of Re complexes and phosphine compounds discussed so far (i.e., structures and dipole moments), we note that reliable results may be obtained by first carrying out a geometry optimization at level IIb (or II for phosphine compounds) followed by a single-point calculation at level IIIb' (or II' for phosphine compounds) for improved energetics. Thus, the subsequent analysis of reaction energies will be based on a combination strategy at level IIIb'/IIb.

3.2. Energetics. 3.2.1. Methodological Aspects. In Table 2 we present the energies for the reactions of Scheme 1 for L = Cp and Cp* as obtained at various levels of computation, and we compared them to experimental reaction energies.¹⁶ Recall that the following basis set study was performed for the Cp model system, while the experimental values correspond to a Cp* ligand; differences between both ligands will be discussed below. The computed values correspond to reactions in the gas phase. To facilitate comparison with experimental data, we have converted the original experimental enthalpy changes ΔH to energy changes ΔE in the gas phase by correcting them for calculated enthalpy contributions and, if applicable,⁶¹ for solvent effects. Later on, we shall separately discuss these corrections which were obtained using the B3LYP method and basis set IIb for rhenium complexes or the equivalent basis set II for the other complexes. For the phosphorus complexes, the effect of the larger basis set II' (which includes d polarization function on the

phosphorus atoms) on the enthalpy corrections was studied for the model compounds PH₃ and PMe₃. Since d polarization functions had only a very small effect (see Table 6), we used basis set II for calculating vibrational frequencies of triphenyl phosphine and of the corresponding oxide.

The experimental enthalpies for reactions C and D were taken from ref 16. For reaction B different values exist in the literature.^{16,50,62} The assumption made in ref 16 concerning indistinguishable heats of fusion and solution for PPh₃ and OPPh₃ seems to be too approximate; see below the calculated solvent effects. Thus, we decided to base the following discussion of reaction energies (including reaction A) on the experimental value of the reaction enthalpy for the P–O bond breaking (B) from ref 50 ($\Delta H = 133.4$ kcal/mol). These authors provide a P–O bond energy that is extrapolated to the gas phase using an estimated value of ΔH_{sub} .⁶³ The data set generated in this fashion will be referred to as Exp.1 (Table 2). However, in Table 2 we also show the original data Exp.2 of ref 16, which are derived with $\Delta H(\text{P–O}) = 136.8$ kcal/mol. Differences between the resulting two data sets will be discussed below.

Hybrid Density Functional Calculations: B3LYP. Comparing experimental and calculated results for the original Cp* system obtained at the most accurate methodological level²⁸ (B3LYP, IIIb'/IIb; Table 2), one finds that the calculated values for the reaction energies A and B deviate from experiment by about 3–6 kcal/mol, or 5%. These errors are quite typical for a hybrid DFT description of transition metal–ligand bonds.²⁸ The energy of reaction C is quite well reproduced, while for reaction D a larger deviation of about 10 kcal/mol is observed. Reaction D may be considered as the sum of the three reactions A, B, and C. Thus the error of the energy of D depends on the errors of A, B, and C. The relative error of the energy D may be quite large since the energies A and B are of comparably large absolute value, but of opposite sign.

Systematic investigations of various methodological aspects were performed for systems with the model ligand Cp; therefore, the following discussion will be restricted to this ligand. Comparing B3LYP energies obtained with different basis sets among each other and with experimental values, it is quite obvious that basis set I (LANL2DZ on all the atoms) is not accurate enough for calculating structures and energies. For example, basis set I does not provide sufficiently accurate structures of hypervalent compounds such as triphenylphosphine oxide. This statement is corroborated by the single-point energies calculated with basis set IIIb'/I (see reaction B in Table 2). Similar deficiencies have previously been reported for transition metal oxo complexes.^{36–38} Optimizations using basis set IIb lead to noticeably improved structures, but calculated energies

(54) Gilheany, D. G. *Chem. Rev.* **1994**, *94*, 1339.(55) Akisin, P. A.; Rambidi N. G. *Soviet. Phys. Cryst.* **1959**, *4*, 334.(56) Reed, A. E.; Schleyer, P. v. R. *J. Am. Chem. Soc.* **1990**, *112*, 1434.(57) Rolke, J.; Brion, C. E. *Chem. Phys.* **1996**, *207*, 173.(58) Magnuson, E. *J. Am. Chem. Soc.* **1990**, *112*, 7940.

are not of completely acceptable accuracy. On the other hand, energies computed with the combination procedure IIIb'/Iib agree well enough with experimental data to corroborate our previous conclusion that structures calculated with basis set Iib are of good quality. Furthermore, addition of polarization functions (f on Re, d on P; procedure IIIb'/Iib) leads to significant improvements of the calculated energies compared to experiment.

The calculated values for reaction energy **A** (Table 2) underline the importance of polarization exponents on the rhenium center (cf. L = Cp, B3LYP: Iib 97.3 kcal/mol vs IIIb'/Iib 109.2 kcal/mol). The energy for abstracting an oxo ligand from CpReO₃ computed with B3LYP using the basis set scheme IIIb'/Iib reproduces the corrected experimental ΔE value 114.1 kcal/mol very well. The agreement is improved even further if one considers that the result for the model ligand Cp is about 4 kcal/mol smaller than that calculated for L = Cp*, 113.4 kcal/mol. Yet, the limited accuracy of energy values evaluated with basis set Iib is obvious from the result for the model ligand Cp. On the other hand, the experimental value for the Re–O bond energy **A** depends also on the energy of reaction **B**, for which experimental values differ by about 10 kcal/mol.^{16,50,62} Reaction energy **B** for L = Cp* computed with B3LYP using the IIIb'/Iib basis set scheme shows a deviation of about 10 kcal/mol from the closed corrected experimental energy –132.0 kcal/mol.⁵⁰ Augmentation of the basis set by phosphorus d exponents improves the reaction energy by about 6 kcal/mol (cf. Iib, –117.9 kcal/mol, and IIIb'/Iib, –123.8 kcal/mol; note that for reaction **B** these two basis set schemes are equivalent to II and II', respectively). Even reaction energy **C** changes slightly, by about 1 kcal/mol, compared to basis set Iib when calculated with the most flexible basis set IIIb'/Iib. Finally, inspection of Table 2 provides evidence for the difficulty to accurately reproduce reaction energy **D**, the original experimental data.¹⁶ In fact, improvement of the model from L = Cp (–24.0 kcal/mol; basis set IIIb'/Iib) to L = Cp* (–19.9 kcal/mol) leads to a larger deviation from experiment, –28.9 kcal/mol; this is a direct consequence of the permethylation-induced energy change for reaction **A** (see above).

To evaluate the influence of different contraction schemes of the original LANL2DZ basis set on the Re center, we have also performed single-point energy calculations for the Cp model with basis set IIIa. Using structures optimized at level Iib, the result for reaction energy **A**, 108.3 kcal/mol, is quite comparable to that of procedure IIIb'/Iib, 109.2 kcal/mol. Thus, the energy effect of partially decontracting the basis set of the transition metal center (Table 1) is rather moderate in the present context.

Gradient-Corrected Density Functional Calculations: BP86, RPBE. The BP86 reaction energies presented in Table 2 have been obtained by single-point calculations on structures optimized with B3LYP and basis set Iib. In Table 2 we compare results from a BP-ECP calculation to those obtained with the scalar-

relativistic variant of the all-electron LCGTO-DF method⁴² (basis sets IIIb'/Iib and AE/Iib, respectively) and to a scalar-relativistic all-electron (basis set AE/Iib) RPBE calculation performed with the program ParaGauss.⁶⁴ The two BP86 results of reaction energies **A** and **B** (for L = Cp) differ from each other by about 5 kcal/mol, while the energies of **C** and **D** are calculated rather similar. The BP86 energy for reaction **A** differs significantly from experiment.^{16,50} If Cp* is used as a ligand instead of the model L = Cp, the reaction energy **A** increases by about 4 kcal/mol (as for the B3LYP method) to 133.1 kcal/mol (IIIb'/Iib; Table 2). Thus, the error of energy **A** relative to experiment is quite large, 19 kcal/mol, while reaction energy **B** is calculated with acceptable accuracy (2 kcal/mol error for procedure IIIb'/Iib). On the other hand, the BP86 value for the dimerization energy **C** agrees very well with experiment. The calculated energy values for reaction **D** deviate substantially from experiment, by about –15 kcal/mol for the model with L = Cp and –19 kcal/mol for L = Cp*. This error is caused by the fact that the BP86 approach slightly (by 1.6 kcal/mol) favors the Re–O bond over the P–O bond. The difference of the corresponding experimental values is about 18 kcal/mol in favor of the P–O bond; this energy difference is noticeably better reproduced by the B3LYP method (by about 10 kcal/mol for L = Cp*). The various BP86 errors for the reaction energies **A**, **B**, and **C** add up to 19.2 kcal/mol for reaction **D** (–9.7 + 28.4 kcal/mol; Table 2), while the corresponding deviation for the B3LYP method is only 9.0 kcal/mol. Thus, the hybrid B3LYP approach is clearly superior to BP86 for the problem under investigation.

The RPBE functional performs quite satisfactorily. For reaction **A** it yields an energy change that is 10 kcal/mol larger than the corresponding B3LYP value, while for reaction **B** the RPBE and the B3LYP energies almost agree (Table 2). The RPBE difference of the absolute values of reaction energies **A** and **B** is slightly larger than that of the all-electron BP86 calculation, and therefore the overall RPBE reaction energy **D** is too small compared to experiment, even smaller than that of the all-electron BP86 calculation.

Thermodynamic studies of oxygen abstraction involve the energy of oxygen dissociation: $\frac{1}{2}\text{O}_2(\text{g}) \rightarrow \text{O}(\text{g})$. The experimental enthalpy of this reaction is 59.5 kcal/mol.⁶⁵ At level II (for this process equivalent to level IIIb'/Iib) the dissociation energy is calculated to be 60.9 kcal/mol using the B3LYP approach. Applying the enthalpy corrections, one obtains a B3LYP value of 60.1 kcal/mol for the dissociation enthalpy of O₂, in excellent agreement with experiment. The situation is quite different for the BP86 functional, where the oxygen dissociation energy is calculated to be 70.2 kcal/mol and the enthalpy to be 69.0 kcal/mol; this deficiency is well documented.⁴⁰ The corresponding RPBE energy value is only slightly improved, 66.9 kcal/mol.⁴³ To eliminate the consequences of this deficiency in the present context, we have also evaluated the reaction energies for Scheme 2 (see Table 7), which is based on modified reactions **A'**

(63) Bedford, A. F.; Mortimer, C. T. *J. Chem. Soc.* **1960**, 1622.

(64) Belling, T.; Grauschopf, T.; Krüger, S.; Nörtemann, F.; Stauffer, M.; Mayer, M.; Nasluzov, V. A.; Birkenheuer, U.; Rösch, N. *ParaGauss 1.9*; Technische Universität München, 1998.

(65) Wagman, D. D.; Evans, W. H.; Parker, V. B.; Schumm, R. H.; Halow, L.; Bailey, S. M.; Churney, K. L.; Nutall, R. L. *J. Phys. Chem. Ref. Data* **1982**, 11, Suppl. 2, p 2.

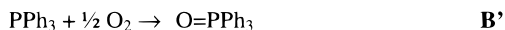
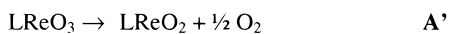
(59) Burrus C. A. *J. Chem. Phys.* **1958**, 28, 427.

(60) Lide, D. R.; Mann, D. E. *J. Chem. Phys.* **1958**, 29, 914.

(61) Quoted experimental values for the P–O bond energy are extrapolated to the gas phase.

(62) Holm, R. H. *Chem. Rev.* **1987**, 87, 1401.

Scheme 2



and **B'** that are reformulated to involve O₂ instead of free oxygen species. Therefore, these energy values are not affected by the erroneous BP86 total energy of the oxygen atom. Comparing BP86 values for L = Cp, we note that the differences between the result of the ECP approach (IIIb'/Iib) and the all-electron method (AE/Iib) are partly due to different descriptions of the oxygen atom. For reactions **A'** and **B'** the two BP86 approaches agree with each other within about 2–2.5 kcal/mol, which is quite acceptable given the various methodological differences. When we compare results for Schemes 1 and 2 obtained with procedure IIIb'/Iib, we find that the differences between B3LYP and BP86 energies of reactions **A** and **B** are substantially reduced in absolute value for **A'** (from –20.2 to –10.9 kcal/mol) and **B'** (from 7.7 to –1.6 kcal/mol). Comparing calculated and experimental results for the Cp* system (level IIIb'/Iib; Table 7), one notes that the B3LYP energy for reaction **A'** agrees satisfactorily with experiment (52.5 vs 54.2 kcal/mol); the BP86 energy differs by about 9 kcal/mol. Ultimately, the better description of the oxygen dissociation leads to the superior overall performance of the B3LYP method for the system under investigation. The RPBE energies are comparable to those of the all-electron BP86 calculations. Reaction energy **A'** fortuitously matches the experimental value, while reaction energy **B'** is about 14 kcal/mol smaller (in absolute value).

The Energy of Phosphine Oxidation. For reaction **B'** all methods, B3LYP and BP86 with IIIb'/Iib as well as BP86 and RPBE at level AE/Iib, yield energy values of about –61 ± 2 kcal/mol (Table 7). From the experimentally determined¹⁶ reaction enthalpy for the oxidation of PPh₃, –135.4 kcal/mol (Table 2), a corrected gas-phase energy value of –75.5 kcal/mol (data set Exp.2) can be derived for reaction **B'**, which is at least 12.6 kcal/mol (in absolute value) above the largest calculated results, –62.9 kcal/mol (Table 7). Better agreement with the calculated reaction energies is achieved if the comparison is based on another experimental enthalpy value for the oxidation of triphenylphosphine, –132.0 kcal/mol⁵⁰ (data set Exp.1; Tables 2, 7). From this latter value one deduces an experimental energy for reaction **B'** of –72.1 kcal/mol (Table 7), which deviates by 9.2 kcal/mol from the presumably best computational value, –62.9 kcal/mol (B3LYP IIIb'/Iib; Table 7). The reaction enthalpy of –135.4 kcal/mol¹⁶ was obtained by assuming that the heats of fusion of the solids of PPh₃ and OPPh₃ are equal. Calculation of solvent effects prototypical for environmental effects on model compounds showed that this assumption may be too severe; the present calculations yield a solvation effect for the phosphine oxidation reaction of about 3 kcal/mol (see below). For this reason, the value of the triphenylphosphine oxidation enthalpy of –132.0 kcal/mol⁵⁰ (gas-phase value from a solid-state value that was corrected for Δ*H*_{sub}⁶³) seems preferable and is used as standard reference throughout the present work.

The smaller phosphine compounds PH₃, OPH₃, PMe₃, and OPMe₃ have also been investigated to study their

possible use as models for triphenylphosphine and triphenylphosphine oxide. The energy of the oxygen transfer reaction PMe₃ + O → OPMe₃ in the gas phase has been measured to –139 kcal/mol.⁵⁰ A calculation with basis set II yields a reaction energy of –121.4 kcal/mol (Table 6) and thus exhibits the same deficiency as for the oxidation of triphenylphosphine: the reaction is calculated substantially less exothermic than experiment. Introduction of d orbitals on the phosphorus center (level II'/II) reduces the error to about 11 kcal/mol. If one compares the calculated reaction energies among each other, one notes that simple phosphine PH₃ with an oxidation energy of –105.2 kcal/mol provides a rather poor model for the oxidation of PPh₃ (–123.8 kcal/mol), whereas PMe₃ with a reaction energy of –127.6 kcal/mol represents a very reasonable model. This result is in line with earlier findings that PMe₃ furnishes an economic model for the energetics of PPh₃.⁶⁶

Enthalpy Corrections. Enthalpy corrections (for T = 298.15 K) with zero-point energies included were evaluated with basis set II (or Iib for Re compounds). Before doing so, we checked the accuracy of this basis set in some detail for the phosphine oxidation reaction **B**, where we also studied the effect of the larger basis set II' on the enthalpy correction. To this end, we compared enthalpy corrections for the model complexes PH₃, OPH₃, PMe₃, and OPMe₃ at the levels II and II'/II (Table 6). Since polarization functions on phosphorus (level II'/II) turned out to have a negligible effect on the enthalpy corrections of the oxidation reaction of the two models PH₃ and PMe₃ (at most 0.4 kcal/mol, Table 6), we restricted these calculations on the triphenylphosphine compounds to level II. From the results of Table 6 one notes that the exothermicity of the reaction O + PH₃ → OPH₃ decreases by about 3.0 kcal/mol when the enthalpy corrections are applied. However, the enthalpy corrections do not vary much when the phosphine substituents are changed to methyl (1.9 kcal/mol) or phenyl (2.1 kcal/mol). The difference between PH₃ on one hand and PMe₃/PPh₃ on the other derives from the fact that vibrational effects involving the oxygen atom are less noticeable in a compound that contains fewer atoms. Taking these results into account, we used vibrational frequencies calculated at level II (or Iib) to derive (hypothetical) experimental reaction energies Δ*E* for the reactions **A**, **B**, **C**, and **D** (as well as **A'** and **B'**) displayed in Tables 2 and 7 from the corresponding experimental reaction enthalpy values Δ*H*.

Solvation Effects. We start the discussion of electrostatic solvent effects with the phosphine oxidation reaction **B**. According to the calculations for the model phosphines PH₃ and PMe₃ (Table 6), solvation effects increase the exothermicity of the oxidation PR₃ + O → OPR₃ by 2.5 and 3.5 kcal/mol for R = H and Me, respectively. (Recall that basis set II'/II is equivalent to the reference procedure IIIb'/Iib, Table 6.) Here, the oxygen atom is assumed to exhibit no solvent effect. We expect static solvent effects on the oxidation of triphenylphosphine (reaction **B**, Scheme 1) to be similar to those computed for trimethylphosphines since the dipole moments of PPh₃ and PMe₃ are quite comparable, and so are the dipole moments of OPPh₃ and OPMe₃ (Tables 4, 5). The larger size of the Onsager cavity of PPh₃ and

(66) Häberlen, O. D.; Rösch, N. *J. Phys. Chem.* **1993**, *97*, 4970.

Table 7. Comparison of Experimental Energies (in kcal/mol) of the Reaction Steps of Scheme 2 with Computational Results Obtained with Various Basis Sets^a and Exchange–Correlation Functionals

	L = Cp				L = Cp*			
	B3LYP	BP86		RPBE	B3LYP	BP86	Exp.1 ^b	Exp.2 ^c
	IIIb'/IIb	IIIb'/IIb	AE/IIb	AE/IIb	IIIb'/IIb	IIIb'/IIb		
A'	48.3	59.2	56.6	54.2	52.5	62.9	54.2	57.6
B'	-62.9	-61.3	-59.2	-58.5	-62.9	-61.3	-72.1	-75.5

^a See Table 1. AE: all-electron calculation (see text). ^b Reaction energies based on data set Exp.1 (see Table 8). ^c Reaction energies based on data set Exp.2 (see Table 8).

Table 8. B3LYP Calculated Reaction Energies ΔE , Temperature and Zero-Point Energy Corrections $\Delta^2 H$, and Solvent Effect $\Delta^2 E(\text{Solv})$ as Well as Comparison of Calculated and Experimental Enthalpies of the Reaction Steps of Scheme 1 for L = Cp* (in kcal/mol)

	ΔE^a	$\Delta^2 H^b$	$\Delta^2 E(\text{Solv})^b$	ΔH				
				calc	Exp.1	Δ^c	Exp.2 ^d	Δ^c
A	113.4	-1.1	0.4	112.7	113.4 ^e	0.7	116.8	4.1
B	-123.8	2.1	-3.5	-125.2	-133.4 ^f	-8.2	-136.8	-11.6
C	-9.5	0.4	2.2	-6.9	-8.4 ^d	-1.5	-8.4	-1.5
D	-19.9	1.4	-0.9	-19.4	-28.4 ^d	-9.0	-28.4	-9.0

^a Procedure IIIb'/IIb. ^b Estimated with L = Cp and basis set II(b); see text. ^c Error of the calculated result compared to experiment. ^d Ref 16. ^e Derived from the other values of this column. ^f Ref 50.

OPPh₃ compared to PMe₃ and OPMe₃ would lead to smaller solvent effects, but the quadrupole contribution is likely larger for PPh₃ because the π systems of the phenyl ligands permit a better electron delocalization.⁵⁰ Therefore, we estimate the solvent effect of reaction **B** from the value calculated for the model PMe₃, -3.5 kcal/mol (Table 6).

Solvation energies have also been computed for the rhenium complexes CpReO₃ and CpReO₂, -4.9 and -4.5 kcal/mol, respectively. Thus, the solvent effect on the energy of reaction **A** is very small, 0.4 kcal/mol. The calculated solvation energy agrees very well the experimental value reported for Cp*ReO₃, -4.5 \pm 0.1 kcal/mol.¹⁶ The solvation energy of the dimer (CpReO)₂(μ -O)₂ is calculated to be -4.6 kcal/mol, from which a solvent effect of 2.2 kcal/mol is derived for reaction energy **C**. Thus, electrostatic solvent effects do not induce important changes in calculated energies of reactions that involve rhenium complexes. From the values discussed, the solvent effect on the overall reaction **D** is estimated to be very small, -0.9 kcal/mol.

Comparison of Calculated and Experimental Reaction Enthalpies. Finally, we compare in Table 8 calculated and experimental enthalpies of the reactions of Scheme 1 with L = Cp*. The calculated values are based on reaction energies obtained at the B3LYP level with the reference strategy IIIb'/IIb; see above for the procedures used to calculate zero-point energy and solvent corrections. The enthalpies calculated for reactions **A**, **B**, and **C** agree very well with the experimental values of data set Exp.1, which is based on the experimental enthalpy of the oxidation of PPh₃ taken from ref 50. All errors are of the same sign and thus accumulate to a large relative error of the overall reaction **D**. Agreement between calculation and experiment is somewhat worse for data set Exp.2, which is based on the experimental enthalpy of P–O bond formation of ref 16.

3.2.2. Chemical Aspects. Abstraction of an oxo group from CpReO₃ by the oxophilic compound PPh₃ according to Scheme 1 (**A** to **D**) is calculated to be overall exothermic by about 25 kcal/mol (20 kcal/mol calculated and 30 kcal/mol experimental for Cp*ReO₃) (Table 2). Formation of the stable dimer (CpReO)₂(μ -O)₂ contributes about 10 kcal/mol to the exothermicity, while the remainder is due to the difference in bond strength between the metal–oxygen bond in CpReO₃ and the phosphorus–oxygen bond in PPh₃. To analyze the effect of the ligand L on the Re–O bond in complexes of the type LReO₃, we calculated the corresponding bond dissociation energy (BDE) also for L = CH₃, C₆H₅, Cl, F, OH, and NH₂ using the B3LYP approach and the reference basis set scheme IIIb'/IIb (Table 9). The energies cover a broad range from Cp (109.2 kcal/mol) to CH₃ (152.7 kcal/mol). The ligands can be classified into three groups of similar BDEs: strong σ /weak π donor ligands (CH₃, C₆H₅), intermediate σ / π donor ligands (Cl, F, OH, NH₂), and moderate σ /good π donor ligands (Cp*, Cp).

The Re–O bond dissociation energy clearly depends on the donor capability of the ligand L, which we will describe in its anionic form L⁻. In the following analysis we will use the Kohn–Sham energies $\epsilon_D(\sigma)$ and $\epsilon_D(\pi)$ of the σ and π donor levels of L⁻, respectively, as measure of their donor (basicity) strength (see Table 9).⁶⁷ Therefore some remarks on orbital energies of anions are in order. All commonly used exchange–correlation functionals fail for very small anions; for example, calculations with GTO basis sets result in occupied levels of positive energy. These problems do not imply that DFT itself fails for anions,⁶⁹ but they are a consequence of fact that all local approximations (including gradient-dependent functionals) provide only insufficient correction of the self-energy error. This results in a wrong asymptotic behavior of the exchange–correlation potential, which in some systems is not attractive enough to bind the additional electron of the anion. To bypass these problems, we stabilized the anions by water as a solvent; that is, we applied a self-consistent reaction field treatment^{32,70} ($\epsilon = 78.54$) which leads to properly bound occupied orbitals for all ligand anions considered and used the resulting orbital energies. For example, CH₃⁻ with its high-lying σ -donating orbital, $\epsilon_D(\sigma) = -2.30$ eV, is a stronger σ donor than Cp⁻, in which the negative charge is delocalized over the π system, which results in a lower lying donor level, $\epsilon_D(\sigma) = -7.72$ eV

(67) Parr, R. G.; Yang, W. *Density Functional Theory of Atoms and Molecules*; Oxford University Press: New York, 1989.

(68) Galbraith, J. M.; Schaefer, H. F., III. *J. Chem. Phys.* **1996**, *105*, 862.

(69) Röscher, N.; Trickey, S. B. *J. Chem. Phys.* **1997**, *106*, 8940. (b) Jaręcki, A. A.; Davidson, E. R. *Chem. Phys. Lett.* **1999**, *300*, 44.

(70) Foresman, J. B.; Keith, T. A.; Wiberg, K. B.; Snoonian, J.; Frisch, M. J. *J. Phys. Chem.* **1996**, *100*, 16098.

Table 9. Calculated Re–O Bond Dissociation Energies^a (in kcal/mol), Bond Lengths *d* (in Å), and Stretching Frequencies ν (in cm⁻¹); Selected NBO Charges *q* (in e) and Dipole Moment μ (in D) of the Complexes LReO₃ for Various Ligands L; and the Energies $\epsilon_D(\sigma)$ and $\epsilon_D(\pi)$ of the σ and π Donor Orbitals of the Ligand in Anionic Form, L⁻ (in eV)

L	BDE	<i>d</i> (Re–O)	ν (Re–O) ^b	<i>q</i> (L)	<i>q</i> (Re)	$\Sigma q(O)$	μ	$\epsilon_D(\sigma)^c$	$\epsilon_D(\pi)$
Ligated Complexes									
CH ₃	152.7	1.715	1017, 982	-0.23	2.06	-1.83	3.09	-2.30	-7.15
Ph	148.5	1.718	999, 970	-0.22	2.06	-1.84	4.86	-3.05	-5.00
Cl	137.5	1.709	1023, 979	-0.28	2.00	-1.71	1.48	-5.51	-5.51
F	136.1	1.707	1031, 986	-0.51	2.31	-1.80	0.96	-4.19	-4.19
OH	135.7	1.713	1018, 978	-0.40	2.26	-1.86	3.34	-4.02	-2.71
NH ₂	132.2	1.718	1006, 971	-0.29	2.16	-1.87	4.42	-4.13	-1.89
Cp*	113.4	1.741	940, 904	-0.02	1.91	-1.89	6.49	-6.69	-2.92
Cp	109.2	1.731	965, 929	-0.15	1.89	-1.74	5.50	-7.72	-3.59
Unligated Complexes ^d									
ReO ₃ ⁻	187.3	1.741	981, 939		0.73	-1.73	0.0		
ReO ₃	154.1	1.715	1017, 973		1.23	-1.23	1.87		
ReO ₃ ⁺	128.0	1.692	1085, 1019		1.61	-0.61	4.24		

^a B3LYP approach with basis set scheme IIIb/IIb. ^b Symmetric and antisymmetric vibration. ^c Solvated free ligand anion L⁻ (water, $\epsilon = 78.54$) calculated with a self-consistent reaction field method. ^d Ligand-free systems; ReO₃ calculated with the unrestricted B3LYP method.

(Table 9). On the other hand, Cp⁻ with its high-lying HOMO π level, $\epsilon_D(\pi) = -3.59$ eV, acts as a good π donor, whereas the π donor capabilities of CH₃⁻ are weak, $\epsilon_D(\pi) = -7.15$ eV (Table 9).

The variation of the Re–O BDE with the various ligands is the result of two factors that influence the bond energy in opposite fashion: (i) the donor–acceptor orbital interaction between the moieties L⁻ and ReO₃⁺, and (ii) the different capabilities of the “reactant” fragment ReO₃ and the “product” fragment ReO₂ to stabilize that transferred electron charge. To reflect this complication, we will in the following differentiate between the Re–O bond order, which is a property of the complex LReO₃ alone, and the Re–O BDE, which is a characteristic that also involves the product LReO₂.

To rationalize the effect of the σ/π donor ability of the ligand fragment L⁻, it is useful to recall the shape of the corresponding accepting orbitals of the fragment ReO₃⁺. The three lowest lying unoccupied orbitals of ReO₃⁺ feature a π antibonding Re–O interaction. The LUMO, with a strong Re $d(z^2)$ contribution, is a σ acceptor orbital, while the next two orbitals, with strong Re $d(xz, yz)$ contributions, are π acceptor orbitals. Obviously, coordination of a ligand with good σ and π donor quality should result in a significant weakening of the Re–O bonds. The higher the energy of the donor level(s) of fragment L⁻, the stronger the donor–acceptor orbital interaction, which increases the population of Re–O π antibonding acceptor orbitals; this entails a weakening of the Re–O bond order and is expected to reduce the Re–O BDE. Inspection of Table 9 reveals that ligand–metal π donation essentially follows this argument: the stronger the π donation capability of ligand L (as measured by the energy of the corresponding orbital), the weaker is the Re–O bond; note that the ordering of the ligands Cp and Cp* does not conform to chemical expectation. However, this straightforward orbital argument fails completely for the σ interaction channel: the higher the donor orbital, the larger the Re–O BDE; see Table 9.

The frequencies of the Re–O stretching vibrations (symmetric and antisymmetric) of the complexes LReO₃ are in line with the analysis of the Re–O bond order (!). From IR and Raman (R) spectroscopic data, one deduces a higher Re–O triple-bond character for CH₃-

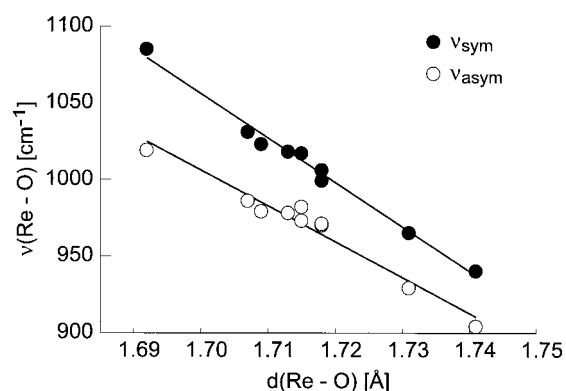


Figure 3. Stretching frequencies $\nu(\text{Re–O})$ (in cm⁻¹) as function of the bond distance $d(\text{Re–O})$ (in Å). Because of the different symmetry (D_{3h}), ReO₃⁻ does not fit the correlation and is thus not shown.

ReO₃ than for Cp*ReO₃ (force constants $\kappa = 8.16$ and 6.99 mdyn/Å, respectively²⁴). The measured frequencies of CH₃ReO₃ are 998 cm⁻¹ (IR), 993 cm⁻¹ (R) for the symmetric Re–O stretching and 947 cm⁻¹ (IR), 941 cm⁻¹ (R) for the antisymmetric stretching. These trends are reproduced by B3LYP calculations at level IIb/IIb. One calculates 1017 and 982 cm⁻¹ for the symmetric and antisymmetric Re–O stretching of CH₃ReO₃; the averaged force constant is $\kappa = 8.99$ mdyn/Å. For CpReO₃ the corresponding calculated values are 965 and 929 cm⁻¹ for the symmetric and antisymmetric Re–O stretching, respectively; the averaged force constant is $\kappa = 8.04$ mdyn/Å. In fact, the stretching frequencies $\nu(\text{Re–O})$ (symmetric and antisymmetric) and the bond distance $d(\text{Re–O})$ of the complexes LReO₃ correlate very well (Figure 3): the longer the Re–O distance, the lower the corresponding stretching frequencies.

Given the failure described above to rationalize the Re–O BDE by orbital arguments alone, a second (independent) factor affecting the Re–O binding energy has to be at work, namely, the charge stabilizing capability of the complexes LReO₃ and LReO₂.

As a first model for the effect of charge variation on the Re–O BDE, one may compare differently charged forms of the fragment ReO₃^q ($q = -1, 0, 1$) which follow the pattern of “longer but stronger bonds”; see Table 9. This latter concept was coined to describe experimental

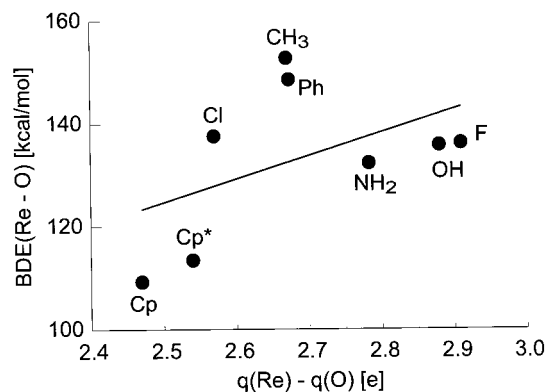


Figure 4. Re–O bond dissociation energy (BDE, in kcal/mol) as a function of the polarity of the bond as measured by the charge difference $q(\text{Re}) - q(\text{O})$ (in e).

observations that also have been verified computationally, e.g., for metal–phosphorus bonds in transition metal complexes involving various substituted phosphine ligands.⁷¹ In the series ReO_3^+ , ReO_3 , and ReO_3^- , the Re–O BDE increases from 128 to 154 and 187 kcal/mol (Table 9), whereas the Re–O distance is elongated from 1.69 to 1.72, and 1.74 Å, respectively (Table 9), in accordance with the fact that a Re–O π antibonding orbital is being filled. From an analysis of orbital interactions alone (as well as of bond distances and vibrational frequencies), these opposite trends seem puzzling. In fact, the reactant fragment ReO_3^q features a significantly stronger electron affinity than the corresponding product species ReO_2^q (ReO_3^+ 10.65 eV, ReO_2^+ 9.52 eV; ReO_3 3.43, ReO_2 2.00 eV). The differences between these electron affinities of about 1.1 eV \approx 26 kcal/mol in the first and 1.4 eV \approx 33 kcal/mol in the latter case are exactly the differences $\text{BDE}(\text{ReO}_3) - \text{BDE}(\text{ReO}_3^+)$ and $\text{BDE}(\text{ReO}_3^-) - \text{BDE}(\text{ReO}_3)$.

After analyzing this model, we now return to the discussion of the Re–O BDE in the complexes LReO_3 . Therefore, according to the argument based on the electron affinity of the fragments, one expects that a ligand L that pushes more electron density on the ReO_3 fragment will not decrease but increase the Re–O BDE of LReO_3 , at variance with the orbital interaction analysis. In fact, the calculated BDE ordering of the ligands Cp and Cp* can be rationalized by this electron affinity argument. Thus, although the ligand Cp* ($q = -0.02$ e; Table 9) donates more electron density to the ReO_3 moiety than the ligand Cp ($q = -0.15$ e) and concomitantly exhibits a slightly longer Re–O bond (1.74 vs 1.73 Å), it features a stronger Re–O BDE, 113 vs 109 kcal/mol. This finding corroborates our Re–O bond analysis of LReO_3 complexes.

Finally, it is worth noting that the Re–O BDE correlates quite well with the charge separation in the Re–O bond, $q(\text{Re}) - q(\text{O})$, which measures the bond polarity: the larger this charge separation, the larger is the Re–O bond energy (Figure 4).

Stabilization of LReO_2 . As stated above, the intramolecular stabilization of the ReO_2 fragment by the ligand L in the LReO_2 complex is important for the

overall energy of oxygen abstraction. This compound is also stabilized in intermolecular fashion, for example by dimer formation through interaction with a second LReO_2 unit. Not unexpectedly, the energy of dimerization is somewhat larger for CH_3ReO_2 (–25.8 kcal/mol) than for CpReO_2 (–9.4 kcal/mol). The difference of about 16 kcal/mol contributes significantly to the overall energy change; it can, at least in part, be rationalized by a direct rhenium–rhenium interaction in $(\text{CH}_3\text{ReO})_2(\mu\text{-O})_2$ which does not occur in $(\text{CpReO})_2(\mu\text{-O})_2$ due to the rather different metal–metal distance. In $(\text{CH}_3\text{ReO})_2(\mu\text{-O})_2$ the Re–Re distance is calculated to 2.59 Å compared to 3.14 Å in $(\text{CpReO})_2(\mu\text{-O})_2$. However, this favorable dimerization energy is not able to compensate the much stronger Re–O bond in MTO (about 43 kcal/mol more than in the Cp analogue). Thus, in case of $\text{L} = \text{CH}_3$, the overall energy of reaction **D** is endothermic, by +3.1 kcal/mol. However, there is experimental evidence that a reaction between MTO and tertiary phosphines occurs in a different manner, as indicated in Scheme 1.^{9,10} MTO may also directly react with the phosphine to give an adduct of the type $\text{CH}_3\text{ReO}_2 \cdot \text{O} = \text{PPh}_3$, where phosphine oxide acts as a stabilizing donor ligand to the LReO_2 fragment. At the B3LYP level, formation of the adduct complex $\text{CH}_3\text{ReO}_2 \cdot \text{O} = \text{PMe}_3$ between MTO and PMe_3 (as model of PPh_3) is calculated to be exothermic, by –12.4 kcal/mol. This value is rather similar to the energy of the analogous reaction of CpReO_3 , –16.9 kcal/mol. Thus, in both cases phosphine will attack and activate an oxo group. However, there is a significant difference between the two phosphine oxide adducts $\text{LReO}_2 \cdot \text{O} = \text{PMe}_3$. For $\text{L} = \text{CH}_3$, the bond between the two fragments is very strong (–37.4 kcal/mol), while it is only –1.5 kcal/mol in the case of $\text{L} = \text{Cp}$. Therefore, for $\text{L} = \text{CH}_3$, phosphine is unable to completely abstract oxygen from LReO_3 , but in the case of $\text{L} = \text{Cp}$ phosphine oxide can be expelled from the complex and the fragment CpReO_2 will be stabilized via dimerization.

4. Conclusions

The present work demonstrates that a quantitative computational description of the thermochemistry of oxygen transfer between a transition metal complex and a substrate is feasible, but several factors have to be taken into account in order to achieve satisfactory results. Attempts to model large compounds by simpler ones (e.g., Cp^*ReO_3 by MTO or PPh_3 by PH_3 or PMe_3) were not successful if high accuracy is required. Nevertheless, investigation of such “model complexes” can yield significant understanding of the electronic structure and metal–ligand bonding of the various species involved in the reaction scheme.

The accuracy of the results was shown to depend strongly on the DFT method chosen and the basis set used. Results calculated with the B3LYP hybrid method agree favorably with experiment, whereas the gradient-corrected BP and RPBE exchange–correlation functionals have been shown to be notably less accurate. Also, f polarization functions on the metal center improve the results substantially; here, we used two f exponents on rhenium. Improved agreement with experiment is achieved when enthalpy corrections and solvation energies are taken into account and flexible basis sets are

(71) Ernst, R. D.; Freeman, J. W.; Stahl, L.; Wilson, R. D.; Arif, A. M.; Nuber, B.; Ziegler, M. L. *J. Am. Chem. Soc.* **1995**, *117*, 5075. (b) Bowmaker, G. A.; Schmidbaur, H.; Krüger, S.; Rösch, N. *Inorg. Chem.* **1997**, *36*, 1754.

used for the ligands. Nevertheless, while in general very good results were obtained with the B3LYP method, this study demonstrated that even for this level of computation it is difficult to achieve an accurate description of the energetics of oxygen transfer reactions. In passing we note that hypervalent molecules such as phosphine oxides require a flexible basis set that includes several d polarization exponents.

Most important for a satisfactory description of the various reaction energies was the use of extended basis sets and realistic ligands, not just simplified model ligands. With such optimum conditions deviations of computed reaction energies from experiment of about 5% or better can be achieved for single reaction steps where strong bonds are formed or broken. However, for the overall reaction scheme, where several energies of opposite signs enter, larger relative errors may occur (see Scheme 1 and Table 2).

With the B3LYP hybrid DFT method the calculated energy of a Re–O bond in the complexes $LReO_3$ (for $L = CH_3, C_5H_6, Cl, F, OH, NH_2, Cp^*,$ and Cp) was shown to strongly depend on the type of ligand. While for CH_3 the bond dissociation energy (BDE) is 152.7 kcal/mol, for Cp it is only 109.2 kcal/mol. Although the ligands Cp^* and Cp coordinate in a fashion rather similar to the metal center, they exhibit small differences in Re–O bond energy and bond type (Cp^* 113.4 and Cp 109.2 kcal/mol); in the Cp compound the bond is 4.2 kcal/mol weaker and less ionic. The differences in the Re–O BDE over the whole series of compounds are controlled by two factors: the orbital interaction between the σ/π donor orbitals of the ligands with its appropriate ac-

cepting orbitals of the ReO_3 fragment and the different electron affinity of the fragments ReO_3 and ReO_2 . The accepting orbitals of the ReO_3 moiety have π antibonding Re–O character. Thus, stronger orbital interaction leads to longer Re–O bond distances and lower frequencies of Re–O stretching vibrations. On the other hand, no satisfactory correlation was found between these bonding characteristics and the calculated Re–O BDE. This was rationalized by the lower stabilizing power of the ReO_2 species for electronic charge. This counteracts the orbital stabilization to differing degree. Both effects seem to be reflected in the polarity of the Re–O bond: the larger the charge separation, the higher the BDE; however, there are some exceptions to this overall trend. With respect to reaction **D** of Scheme 1, one notes that in CH_3ReO_3 the Re–O bond is so strong that an oxygen atom cannot be totally abstracted by PR_3 , as is the case for Cp^*ReO_3 . However, in CH_3ReO_3 the Re–O bond may be activated through a phosphane base, resulting in the complex $CH_3ReO_2 \cdot O=PR_3$, while for the Cp^* derivative the phosphine oxide is extruded from the complex and the resulting Cp^*ReO_2 is stabilized by dimerization, forming $(Cp^*ReO)_2(\mu-O)_2$.^{9,10}

Acknowledgment. We thank P. Hofmann, F. Kühn, and C. R. Landis for stimulating discussions. This work was supported by the Deutsche Forschungsgemeinschaft, the Bayerischer Forschungsverbund Katalyse (FORKAT), the German Bundesministerium für Bildung, Wissenschaft, Forschung und Technologie (No. 03D0050B), and the Fonds der Chemischen Industrie.

OM9904854